EUROPHYSICS LETTERS 15 February 2002

Europhys. Lett., **57** (4), pp. 499–505 (2002)

Grazing-incidence diffraction anomalous fine structure of InAs/InP(001) self-assembled quantum wires

S. Grenier[1], M. G. Proietti[2], H. Renevier[1], L. González[3], J. M. García[3] and J. García[2]

[1] *Laboratoire de Cristallographie, CNRS - B.P. 166, 38042 Grenoble Cedex 09, France*
[2] *Departamento de Física de la Materia Condensada, Instituto de Ciencia de Materiales de Aragón, CSIC-Universidad de Zaragoza - c. Pedro Cerbuna 12, 50009 Zaragoza, Spain*
[3] *Instituto de Microelectrónica de Madrid, CSIC*
c. Isaac Newton 8, 28760 Tres Cantos, Spain

(received 29 May 2001; accepted in final form 20 November 2001)

PACS. 61.10.-i – X-ray diffraction and scattering.
PACS. 61.10.Ht – X-ray absorption spectroscopy: EXAFS, NEXAFS, XANES, etc.
PACS. 68.65.-k – Low-dimensional, mesoscopic, and nanoscale systems: structure and non-electronic properties.

Abstract. – We have studied nanostructured samples of InAs/InP(001) by means of Grazing Incidence Diffraction Anomalous Fine Structure. The samples, grown by molecular beam epitaxy, show a periodic corrugation on the surface giving rise to an array of self-assembled quantum wires after deposition of 2.5 monolayers of InAs. We measured the (440) and (420) GIDAFS spectra, at the As K-edge, at incidence and outgoing angles close to the substrate's critical angle. We analysed the anomalous diffraction lineshapes *vs.* the energy, as well as the oscillatory part of the signal in the extended region above the edge and obtained, for the first time, information about composition and strain *inside* the quantum wires and *close* to the interface. Our results suggest possible interfaces.

Introduction. – InAs nanostructures on InP(001) are candidates for light-emitting devices in the wavelength range of 3–1.55 μm. Arrays of crystalline quantum wires (QWrs) can arrange spontaneously during the first steps of epitaxial growth on the InP substrate. The nanostructures auto-organization is driven by the strain at the interface due to the lattice mismatch between substrate and epilayer. The interface formation mechanisms are known to be quite complex and strongly dependent on growth conditions, substrate temperature, group-V flux, surface reconstruction, buffer layer surface morphology, and other effects [1, 2]. The quantum arrays are characterized mainly in terms of optical (luminescence, photoreflectance) and vibrational (Raman) properties, while Atomic Force Microscopy (AFM) and Transmission Electron Microscopy (TEM), that are local probes, give the shape and qualitative information on the homogeneity of the islands. The statistic strain and composition of the nanostructures and interfaces with the substrate are indeed the subject of intense investigations, since reactions with the substrate atoms or segregation mechanisms of the impinging species can occur. The knowledge of these parameters is mandatory for the understanding of the growth mechanism and the self-assembling as well as of the electronic and opto-electronic properties of the nanostructures.

In the present paper we report the study of InAs QWrs formed on InP(001) substrate by means of Grazing Incidence Diffraction Anomalous Fine Structure. The DAFS measurements

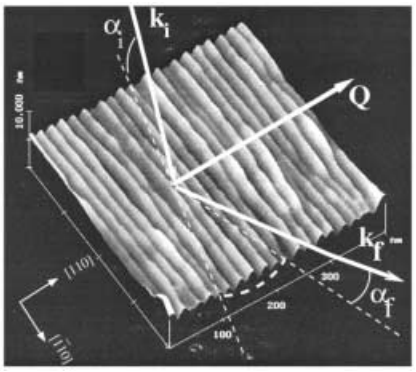

Fig. 1 – AFM tridimensional view of InAs QWrs on InP buffer from [2] with a scheme of the glancing angle diffraction measurement.

were carried out at grazing incidence and outgoing angles close to the critical angle of InP, to enhance the contribution of the very thin epilayer with respect to the substrate. The method offers the unique advantage of combining the chemical selectivity of Extended X-Ray Absorption Fine Structure (EXAFS) with the spatial and site selectivity of X-Ray Diffraction (XRD) [3]. Thanks to the QWrs short-range periodicity that gives rise to broad satellites in the reciprocal space, the spatial selectivity was achieved by choosing a momentum transfer vector, $\overrightarrow{Q}$, at the maximum intensity of a satellite peak. The As local environment was probed by tuning the incident beam at the As K-edge and by measuring the diffraction fine structure as a function of the energy at constant $\overrightarrow{Q}$ vector. It should be noted that P substitute for As, therefore the data analysis would have been easier at the In K-edge; however, we chose not to work at the In K-edge to avoid the substrate contribution through the transmission functions. It is shown, hereafter, that GIDAFS and EXAFS data at the As K-edge are quite different, emphasizing the interest of DAFS for studying these materials.

Experiment. – Samples have been grown by solid source Molecular Beam Epitaxy (MBE) onto InP(001) wafers, after growing a 200 nm thick InP buffer layer. The nominal InAs coverage is of about 2.5 mono-layers (ML). A periodic corrugation of the epilayer is obtained giving place to an array of wires aligned along the $[1\bar{1}0]$ direction, as shown in fig. 1a, with a typical length above 1 μm, a height between 0.6 and 2 nm and a period of 20 nm. Details on growth and characterisation have been published elsewhere [1]. The DAFS measurements were carried out at the French Collaborative Research Group beamline BM02 at the European Synchrotron Radiation Facility. Silicon (111) single crystals were used for beam monochromatisation, giving an energy resolution of about 1 eV at the As K-edge (11.867 keV). The sample was mounted with the electric polarisation vector of the incident beam perpendicular to the sample surface. We performed the GIDAFS measurements in grazing geometry, according to the scheme of fig. 1, with an incidence angle close to 1.5 times the critical angle of InP at 12 keV($\approx 0.3°$), and kept constant during the scan. The spectra were recorded by measuring, as a function of the energy, the maximum intensity of the most intense satellite on the low side of the radial scan (Q_{r}-scan) of the substrate peak (see arrow in fig. 2).

Data analysis. – The DAFS method has the unique capability of providing long-range order crystallographic information together with absorption-like short-range order information. These are contained in the structure factor of the measured Bragg reflection and in the anomalous complex atomic scattering factor *f*. The latter can be split into a smooth and an

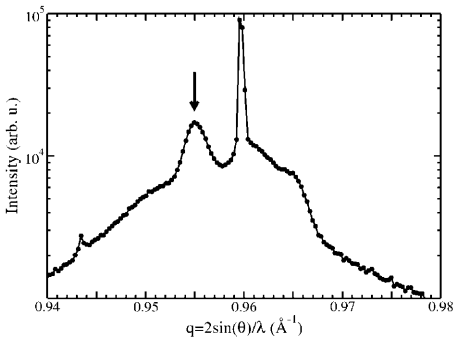

Fig. 2

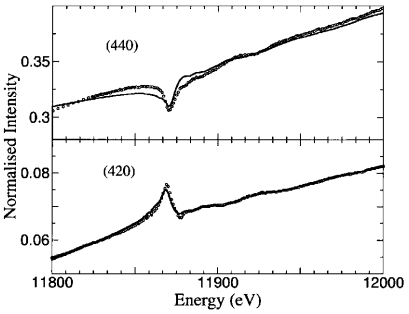

Fig. 3

Fig. 2 – (440) XRD intensity of QWrs sample, as a function of the momentum transfer, recorded in glancing-angle geometry at 11.8 KeV.
Fig. 3 – (440) and (420) Grazing Incidence DAFS spectra of the QWrs sample, at the As K-edge (dotted curves) and crystallographic fits (continuous curves).

oscillatory parts [4]. In the forward-scattering limit:

$$f = f_0\left(\overrightarrow{Q}\right) + f'(E) + if''(E) = f_0\left(\overrightarrow{Q}\right) + f_0'(E) + if_0''(E) + \Delta f_0''\left(\chi'(E) + i\chi''(E)\right),$$

where f_0 is the Thomson scattering term, f_0' and f_0'' are the smooth real and imaginary terms of f, χ' and χ'' are the oscillatory contributions to f' and f'', respectively. The data analysis was performed in two steps. First, a crystallographic co-refinement of the GIDAFS spectra was done using the DPU code [5], details are given in our previous paper [4]. The structure factor was calculated with the crystallographic parameters of the Zinc-Blende structure, allowing P atoms to substitute for As atoms. The Bragg diffracted intensity was corrected for a transmission coefficient, $|T_\mathrm{i}|^2|T_\mathrm{f}|^2$, that represents the effect of refraction, at the substrate surface, of the incoming X-ray wave. We applied the Distorted Born Wave Approximation (DBWA) [6], considering that total reflection takes place essentially at the interface with the substrate, *i.e.* regarding the nano-objects as a small perturbation of the electric field above the substrate. The fit parameters included scale and slope factors to take into account geometrical and detection effects. Other parameters were Debye-Waller factors and the P concentration, x, in $InAs_{1-x}P_x$. The crystallographic simulations, shown in fig. 3 (continuous curves), have been calculated using the experimental (oscillating) f'' of bulk InAs, obtained from the transmission

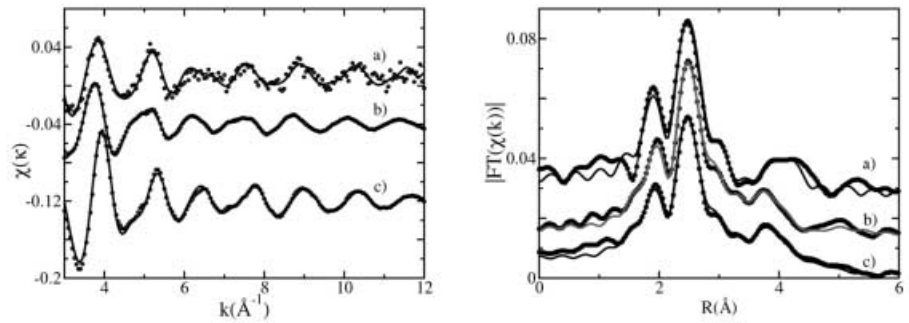

Fig. 4 – Panel (a) Grazing incidence (420) EDAFS of InAs QWrs at the As K-edge (a) compared with the (420) EDAFS of the crystallographic fit (b) and EXAFS of bulk InAs (c). Panel (b) Fourier transforms of the panel (a) spectra. The best fits for each spectra are also shown as continuous curves.

TABLE I – *Best-fit results for the bulk powder InAs EXAFS and the corresponding simulated EDAFS (italic).*

Pair	Distances (Å)	Debye-Waller (Å^2)
As-In (1st shell)	2.616±0.003	0.0040±0.0005
	2.611±0.007	*0.0036±0.0006*
As-As (2nd shell)	4.272±0.005	0.0135±0.0023
	4.264±0.012	*0.0140±0.0026*
As-In-As (MS path)	4.752±0.006	0.0028±0.0024
	4.743±0.013	*0.0044±0.0032*
As-In (3rd shell)	5.009±0.006	0.026±0.0035
	5.000±0.014	*0.027±0.0042*

EXAFS spectrum of a powdered sample. The real part, f', of the scattering factor was calculated by a Kramers-Kronig transformation of f''. Smooth theoretical curves from the Cromer-Libermann tables were used for f' and f'' of In and P atoms. Second, we extract the oscillations above the edge, or extended DAFS (EDAFS), and analyzed them according to the EXAFS data processing scheme, to obtain the local structure parameters, as interatomic distances, coordination numbers and Debye-Waller factors. The EDAFS spectra have been compared with theoretical phase and amplitudes calculated by the FEFF8 code [7], by means of a best-fit procedure performed by the FEFFIT program [8]. The crystallographic fit also provides the EDAFS scale and phase factors that allow to analyze EDAFS as EXAFS data. The data analysis procedure has been described extensively elsewhere [4]. In order to check the reliability of our data analysis method, we performed the fit on the bulk InAs experimental EXAFS spectrum and on the InAs bulk DAFS spectrum calculated starting from EXAFS. The fit results are shown in figs. 4b and c (continuous curves) and in table I. The bulk InAs EXAFS spectrum (fig. 4c, panel a) was fairly fitted by using the standard crystallographic structure parameters for InAs. One multiple scattering path (MS) was not negligible and was included in the fit of the EXAFS and (420) EDAFS spectrum. It corresponds to a triangular three-atom path As-In-As. The same parameters were found, within the uncertainties, for the bulk InAs EDAFS spectrum, as expected.

Results. – Crystallographic structure. The XRD radial scan spectrum of the QWrs sample, recorded at 11.8 keV, around the (440) Bragg reflection of the substrate, is shown in fig. 2. The momentum transfer vector $\overrightarrow{Q}$ is oriented along the [110] direction, *i.e.* perpendicular to the wires. The sharp Bragg peak for $\overrightarrow{Q}$ at about 0.96 Å $^{-1}$ corresponds to the (440) Bragg reflection of the InP substrate. Several satellite peaks due to the wires periodicity clearly appear close to the substrate peak. The satellites' spacing gives a wire periodicity, $\lambda = 1/\Delta Q \approx 200$ Å, in fair agreement with the AFM image. A radial scan of the (420) peak was also recorded and showed a shape very similar to (440). The GIDAFS spectra of the QWrs sample for the (440) and (420) Bragg reflections, as well as the crystallographic fits are shown in fig. 3. A clear result from the fit is that, to reproduce the shape of the anomaly at the edge, we do need to include the presence of P in the epilayer. As a result of the iteration we find a P concentration $x \cong 0.5 \pm 0.1$. This shows that a considerable density of P atoms, with the same periodicity as the wires, is contributing to the satellite diffraction peaks. At this point, diffraction cannot tell if the P atoms participating to the diffraction belong to the wires or to the InP substrate. The latter could show a periodic undulation and/or periodic strained areas due to the strain at the interface with the InAs wires.

Local structure. Now we report on the analysis of the diffraction fine structure. The glancing-angles (420) EDAFS oscillations, after background subtraction, are shown in fig. 4a, panel (a) (dotted curve). They are compared with the EDAFS oscillations of the crystallographic fit, calculated with experimental f'_{As} and f''_{As} of InAs bulk (fig. 4b, panel (a)). The overall behavior of the two DAFS spectra are quite similar, the contribution of the In nearest neighbor (NN) of As is indeed dominant over the contribution of next NN (NNN) that are only As in bulk InAs, and As and P in the QWrs spectrum. Nevertheless, some differences can be observed, out of the noise level of the EDAFS QWrs spectrum. It is more evident in fig. 4, panel (b), by comparing the Fourier Transforms (FT) of the EDAFS spectra. The NN shell contributions are quite similar to each other, whereas the NNN peaks are differents, showing a change in the NNN environment. The best-fit curves for the QWrs sample are shown in fig. 4a (continuous curves), and compared with the experimental EDAFS and FT (dotted curves). All the FTs reported in fig. 4, panel (b) were calculated in the same range 3–11.7 Å^{-1}. The fit was performed on the raw data, in the R-space, in the range 1.5–5.9 Å, by iterating a maximum of 11 parameters. The As-In NN and As-As NNN distances were fixed at the values foreseen by the elastic theory for a pseudomorphic epilayer of InAs grown on InP, *i.e.*, 2.60 Å and 4.29 Å. The As-P NNN distance has been refined and found to be equal to 4.17 Å $\pm$ 0.02 Å. The P concentration, $(1-x)$, was also refined, giving $(1-x) = 0.4 \pm 0.15$. It is, within the errors, equal to the value found by the crystallographic fit of the anomalous diffraction *line-shape* at the edge. The second shell As-P distance is quite short, close to the P-P distance in bulk InP (4.15 Å). Nevertheless, the shapes of the spectra, in k- and R-spaces, were reproduced only when freeing this parameter and letting it vary independently of the As-As distance. The shapes we are referring to correspond to the low-k range oscillations of the *chi* spectrum and the second shell environment in the FT, just below 4 Å, corresponding to the NNN contribution. The intensity of that contribution is much lower in the case of the QWrs in comparison with bulk InAs. It can be reproduced by adding out-of-phase As-P and As-As contributions with an As-P distance of 4.17 Å. We want to note that the polarization of the incoming photons was directed along the (001) direction, *i.e.* perpendicular to the surface, making an angle of 90° with the NNN $\boldsymbol{R}_{ij}$ vector from the As absorber to the As (P) atoms lying in the (001) plane (in-plane NNN). Therefore the NNN contribution to EDAFS is due only to the 8 out-of-plane NNN atoms at a distance, according to elasticity, of 4.29 Å from the As absorber. The in-plane NNN As atoms should instead show a distance, in the case of a perfect pseudomorphic layer, equal to the P-P NNN distance of InP bulk, *i.e.* 4.15 Å. Qualitative inspection of our XRD measurements as well as previous results [9] indicate a weak relaxation along the [110] direction. An upper limit to relaxation can be given by the XRD spectrum in fig. 2, considering the most intense satellite as the maximum of the broad envelope curve supposedly due to the InAs epilayer. From its position in $\overrightarrow{Q}$ we can estimate the lattice parameter and, roughly, a strain of about 2%, instead of 3.2% for the pseudomorphic case. According to elasticity, the As-In distance would change from 2.60 Å to 2.614 Å. Considering that we would see an average between the two values, since the layer shows to be pseudomorphic along the $[1\bar{1}0]$ direction, we should expect to observe a correction to the As-In distance lower than 0.01 Å, that is within the error of our measurement. The same consideration applies to the NNN As-As distance, note that it is 4.29 Å for the strained InAs and 4.27 Å for bulk InAs [10]. We also have to point out that a feature at about 4.5 Å is observed in the QWrs FT spectrum that does not show in the bulk InAs FT. It is reproduced in the fit by the MS In-As-P contribution that is not present in the bulk InAs spectrum, and appears to be quite intense for the QWrs. Measurements with a better signal-to-noise ratio are needed to clarify this effect. In any case it does not affect the evidence of a short As-P distance. Glancing-Angle EXAFS was also measured, on the same

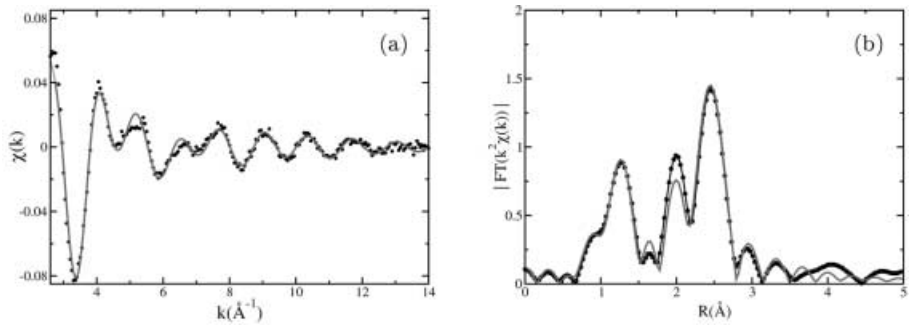

Fig. 5 – (a) Grazing-incidence EXAFS of InAs QWrs. (b) The Fourier tranform, with the best fit as continuous curves, including As-O and As-In single-scattering paths.

QWrs sample, by detecting the As fluorescence yield. The As-In distance was found to be of 2.60 ± 0.03 Å, *i.e.* equal within the error, to the value found by EDAFS. Nevertheless, the surface oxide layer strongly affects the EXAFS spectrum, causing a strong loss of information, in particular for shells beyond the first one (fig. 5). The EDAFS oscillations instead are not affected by the oxide, thanks to the site selectivity of diffraction.

Discussion. – In this work we show that DAFS can be applied, in grazing geometry, to the study of self-assembled nanostructured materials representing an extremely low equivalent coverage of about 2.5 MLs. We performed crystallographic and EDAFS analysis of the (440) and (420) GIDAFS spectra, and compared the information. In particular, we obtained the composition and strain *inside* the wires. The quality of the spectrum may be improved using higher-brilliance beamline, nevertheless the signal-to-noise ratio of our spectra allowed quantitative analysis. We have shown that, in both spectra, we detect the presence of a consistent amount of P atoms, $(1 - x) = 0.4 \pm 0.1$. Does it means that the quantum wires are grown as $InAs_{0.5}P_{0.5}$/InP? We can answer by comparing the values of the interatomic distances with the values found for bulk and superlattice InAsP samples in a recent work [10]. One must note that in our case the polarization vector of the electric field of the X-ray incident beam was perpendicular to surface plane (001), whereas it was in the surface plane in the cited paper. The NNN distance, R_2, for As-As and As-P pairs, reported by the authors, can be approximated by the weighted average of the in-plane and out-of-plane distances, according to the expression

$$R_2 = \frac{N_\perp R_{2\perp} + N_\parallel R_{2\parallel}}{N_\parallel + N_{2\perp}} ,$$

where $N_\perp$ and $N_\parallel$ are the out-of-plane and in-plane coordination numbers, corrected for polarization and finite thickness of the epilayer (for 3 ML, $N_\perp/N_\parallel \cong 4/6$). The values they found at $x \cong 0.4$ for R_2 are about 4.19 and 4.2 Å for As-P and As-As, respectively. We can estimate the out-of-plane NNN distance from the former expression assuming pseudomorphicity, *i.e.* taking $R_{2\parallel}$ as P-P distance in bulk InP (4.15 Å), and using the former experimental R_2 values. We obtain 4.25 and 4.28 Å for $R_{2\perp \mathrm{As-P}}$ and $R_{2\perp \mathrm{As-As}}$, respectively, *i.e.* a NNN distance value for the As-P pair much higher than the value of 4.17 Å, our experimental value. In the case of the relaxed bulk InAsP alloy, we would see the same relaxed NNN distance for the in-plane and out-of-plane atoms. The values found in ref. [10] are 4.26 Å for the As-As pair and 4.22 Å for the As-P pair. The As-P distance is again appreciably longer than the value we have found. This result suggests therefore that, due to the low epilayer thickness and to the X-ray beam polarization, the interface effects on the EDAFS spectrum are remarkable, *i.e.*,

the P atoms contributing to EDAFS have to belong to the interface region between InAs and InP, *therefore the core of QWrs is essentially InAs*. We cannot have an abrupt, atomically flat InAs/InP interface since in that case the P concentration, obtained by EDAFS, measured with [001] polarization, should be $(1-x) \approx 0.3$, due to the fact that the As atoms belonging to the first InAs ML have P atoms of the InP substrate as NN neighbors, at a distance of about 4.20 Å. The value that we find experimentally for P concentration is higher and the As-P distance is shorter. Moreover, no P contribution to the DAFS line-shape at the edge should be found according to this model, whereas the crystallographic fit shows a P concentration close to that found by EDAFS. The high P content seen by diffraction can be explained by an abrupt InAs/InP interface with periodic InP strained regions generated in the InP buffer layer, beneath the wires, or a corrugated InAs/InP interface with the same wires periodicity. The interface formation mechanisms are known to be quite complex. The As atoms can be incorporated indeed, at the InP surface, between 0.5 and 1.5 MLs, during P/As switch prior to In deposition for InAs growth [9]. A sort of corrugation of the InP substrate could be produced by As incorporation on the P-rich buffer layer surface, forming elongated islands along the $[1\bar{1}0]$ direction. This has been observed in AFM studies of the first growth steps of InAs/InP [2]. On the other hand, the short As-P distance is in agreement with a small contraction of the InP lattice parameter in proximity to the interface, due to the tensile strain on InP. Therefore our results suggest that we are observing a corrugated interface and buffer layer deformation at the same time.

* * *

We acknowledge the French CRG-BM02 (D2AM) and the Italian CRG-BM08 (GILDA) beamlines for granting beam time and for technical assistance. We are grateful to Drs. F. D'Acapito and A. Mazuelas for helpful discussions. One of the authors (MGP) is pleased to acknowledge support from the "Université Joseph Fourier" of Grenoble and the "Centre National pour la Recherche Scientifique" for visits during which the research was completed. This work was also supported by the LEA-MANES European Agreement and by CICYT project No. MAT99-0847.

REFERENCES

[1] González L., García J. M., García R., Martinez-Pastor J. and Ballesteros C., *Appl. Phys. Lett.*, (2000) 1104.
[2] Brault J., Ph.D. Thesis, no. 2000-29, Ecole Centrale de Lyon, France (2000); Brault J., Gendry M., Grenet G. and Hollinger G., *Appl. Phys. Lett.*, **73** (1998) 2932.
[3] See, for instance, Hodeau J. L., Favre-Nicolin V., Bos S., Renevier H., Lorenzo E. and Bérar J. F., *Chem. Rev.*, **101** (2001) 1843.
[4] Proietti M. G., Renevier H., Hodeau J. L., García J., Bérar J. F. and Wolfers P., *Phys. Rev. B*, **59** (1999) 5479.
[5] Wolfers P., private communication (Laboratoire de Cristallographie).
[6] Dosch H., *Critical Phenomena at Surfaces and Interfaces*, *Springer Tracts Mod. Phys.*, Vol. **126** (Springer Verlag) 1992.
[7] Ankudinov A. L., Ravel B. and Rehr J. J., *Phys. Rev. B*, **58** (1998) 7565.
[8] Stern E. A., Newville M., Ravel B., Yacoby Y. and Haskel D., *Physica B*, **208&209** (1995) 117.
[9] García J. M., González L., González M. U., Silveira J. P., González Y. and Briones F., *J. Cryst. Growth*, **227-228** (2001) 975.
[10] Pascarelli S., Boscherini F., Lamberti C. and Mobilio S., *Phys. Rev. B*, **56** (1997) 1936.